Theoretical Study of the Excited State Properties and Transitions of 2-Aminopurine in the Gas Phase and in Solution

John M. Jean* and Kathleen B. Hall

Department of Biochemistry and Molecular Biophysics, Washington University School of Medicine, 660 S. Euclid Ave., St. Louis, Missouri 63110

Received: October 28, 1999; In Final Form: January 5, 2000

Ab initio calculations of the vertical transitions, transition dipole moments, and permanent dipole moments of several low-lying valence states of the fluorescent base 2-aminopurine have been obtained in both the gas phase and in water using the configuration interaction singles method in conjunction with the Onsager reaction field model. The results for the electronic state ordering, excited state energy gaps, and transition dipole moment directions are in generally good agreement with those determined experimentally. The fluorescence Stokes' shift for the $S_0 \rightarrow S_1$ transition is computed taking into account the contributions from both intramolecular and solvent reorganization processes. The result is in excellent agreement with experiment and suggests that the magnitude of the shift is due primarily to intramolecular relaxation of the S_1 state.

2-aminopurine (2AP) is a highly fluorescent base that has found extensive use as a site-specific probe of the local structure of oligonucleotides,[1−4] conformational transitions in RNAs,[5] the dynamics of mismatched base pairs,[6] abasic sites in DNA,[7] and DNA duplex melting.[8] It forms a Watson−Crick base pair with thymine,[1,9,10] which makes it a nearly nonperturbative replacement for adenine (6-aminopurine) in DNA; however, it can also weakly pair with cytosine.[11−13]

The high fluorescence quantum yield of 2AP (0.66 in aqueous solution)[14] compared to adenine is a result of the electronic effect of amino substitution at the 2-position of the six-membered ring, which significantly lowers the first $\pi-\pi^*$ transition (S_1) energy placing it well below the $n-\pi^*$ transition.[14,15] In adenine, as in purine, the close proximity of these two states introduces the possibility of rapid nonradiative deactivation of the dipole-allowed $\pi-\pi^*$ state, possibly contributing to its low fluorescence quantum yield. The significantly red-shifted $\pi-\pi^*$ absorption in 2AP not only precludes rapid internal conversion to the $n-\pi^*$ state but also allows for selective excitation of this base even in relatively large nucleic acid structures.

Despite 30 years of experimental studies of 2AP-labeled nucleic acids, few descriptions of its electronic and optical properties exist, either in solution or in the context of a nucleic acid. While the ground-state structure of 2AP has not been determined experimentally, the structure of the derivative, 9-[4-acetoxy-3-(acetoxymethyl)butyl]-2-aminopurine, has been determined by X-ray diffraction.[16] Broo and Holmén have performed ab initio calculations on the 2AP ground state and obtained optimized geometries at the MP2/6-31G(d) and DFT/6-311++G(df,p) levels.[17] The bond angles and distances obtained using these two models agree remarkably well with each other and with those determined for the 2AP derivative. The degree of pyramidalization of the amino group, however, was found to depend slightly on the size of the basis set, with increasing basis size leading to an increasingly planar structure.

The pyramidal amino group geometry and slight distortion of the purine ring from planarity leads to C_1 symmetry for ground state 2AP. One effect of base stacking interactions on 2AP in a labeled RNA or DNA, in addition to possible electronic mixing of the low-lying states with those from neighboring bases, is distortion of the amino group to a (nearly) planar conformation (i.e., $\sim C_s$ symmetry); thus the energetic cost of this distortion and its effect on the excited-state transition energies and dipole moments is of interest.

Interpretation of the electronic spectra of purine and adenine is complicated by the $N_7H \leftrightarrow N_9H$ tautomeric equilibrium.[18] Broo and Holmén found that the N_7H tautomer of 2AP is approximately 11 kJ/mol greater in energy than the N_9H form in aqueous solution, suggesting the latter predominates at room temperature. While substantial evidence exists that both tautomers contribute to the fluorescence spectrum of adenine,[19] the situation in 2AP is unclear. Only recently has experimental data on the electronic manifold of 2AP appeared. Holmén et al. have measured the linear dichroism, magnetic circular dichroism, and fluorescence anisotropy of 2AP and 2AP-riboside oriented in PVA films in order to determine the electronic state ordering, relative energetics, and transition dipole directions of the $\pi-\pi^*$ and $n-\pi^*$ states.[14] Their results showed that the N_9H tautomer is the predominant form (>97%) present, in agreement with the theoretical prediction, and identified several low-lying $\pi-\pi^*$ and $n-\pi^*$ excited states for this tautomer. Recent ab inito calculations suggest that the $N_7H \leftrightarrow N_9H$ equilibrium may be established in the excited state manifold.[15] The multicomponent fluorescence decay of 2AP measured by Santhosh and Mishra is consistent with this;[20] however, Holmén and coworkers found that the excitation energies, fluorescence anisotropies, and transition moments for 2AP and 2AP riboside (which cannot undergo tautomerization) were virtually identical, strongly suggesting fluorescence arising from a single tautomeric species. Regardless of whether the N_7H tautomer plays a role in determining the fluorescence characteristics of 2AP in solution, our primary goal is to fully characterize the spectral properties of 2AP in the context of a nucleic acid. Since binding of 2AP to the sugar−phosphate backbone occurs via N_9, we only consider the N_9H form of 2AP in this study. We also point out that the similarity of the 2AP and 2AP riboside spectral

* To whom correspondence should be addressed. E-mail: jjean@wanda.wustl.edu. Phone: (314) 362-4197.

10.1021/jp9938258 CCC: $19.00
Published on Web 02/05/2000

properties clearly indicate that the sugar has no perturbative influence on the excited state electronic structure.

From the linear dichroism data, the approximate transition energy for the out of plane polarized n−π* transition is 36 000 cm^{-1} (278 nm), which is approximately 3200 cm^{-1} above the $\pi-\pi$* S_1 state (305 nm) and 4000 cm^{-1} below the $\pi-\pi$* S_3 state (250 nm). The electronic state ordering, excitation energies, and transition dipole directions were partially corroborated by semiempirical INDO/S-CI calculations and by recent CIS/6-31G and CASSCF calculations.[14,15]

The work of Holmén et al. provides a reasonably accurate description of the electronic properties of 2AP in a polar condensed phase environment as well as valuable data upon which to judge the accuracy of higher level quantum chemical calculations of the manifold of electronically excited states from the minimum of the ground state (S_0) potential surface. The initial state in the fluorescence transition, however, corresponds to the minimum of the S_1 surface (assuming vibrational relaxation is faster than the excited state lifetime); thus a knowledge of excited state energy gaps, dipole moments, and transition properties at this geometry are important for predicting environmental effects on the 2AP fluorescence spectrum.

In this paper, we report results from ab initio calculations of the vertical transition energies, permanent dipole moments, and transition dipole moments of the lowest-lying $\pi-\pi$* and n−π* states of 2AP both in vacuo and in a dielectric continuum using the configuration interaction singles (CIS) method.[21] In addition, we have performed geometry optimizations of the S_1 state using basis sets containing both polarization and diffuse functions. These results allow us to determine the excited state energy gaps and dipole moments corresponding to the fully relaxed S_1 state and to estimate the relative contributions of intramolecular and solvent reorganization processes to the fluorescence Stokes' shift. Our results provide a thorough, albeit approximate, description of the low-lying valence states of 2AP and provide a reference for interpreting the influence of base-stacking and base-pairing interactions on the structure and properties of the fluorescent state (Jean and Hall, in preparation).

Computational Methods

Ground State Geometries. All calculations were performed using the Gaussian 94 package[22] on an SGI Power Challenge R8000 workstation. Geometry optimizations of 2AP in vacuo were carried out at the MP2/6-31G(d,p) level for the C_1 symmetry structure and at the RHF/6-31G(d,p) and MP2/6-31G-(d,p) levels for the planar C_s structure. The optimized geometry of the C_s symmetry species was obtained by constraining the dihedral angles to their appropriate values of either 0° or 180°.

Excited State Calculations. Vertical transition energies were obtained using the CIS method, which expresses the wave function of a given excited state as a linear combination of singly excited determinants, each obtained from a Hartree−Fock reference determinant (in our case, the determinant corresponding to the ground state) by replacing an occupied spin−orbital with a virtual spin−orbital. The calculations reported here employed the frozen core approximation in which only configurations arising from excitations out of valence orbitals are included. Within this constraint, all singly excited configurations were included in calculating the CI wave functions. To properly account for orbital relaxation effects, permanent dipole moments of the excited state were computed using the CIS density. Geometry optimizations of the S_1 $\pi-\pi$* state were carried out at the CIS/6-31+G(d,p) and CIS/6-31G(d,p) levels in order to test the influence of diffuse (sp) functions on the excited state geometry.

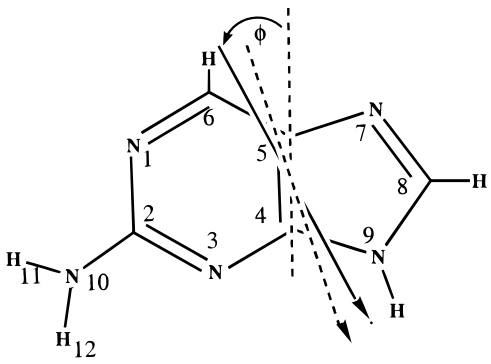

Figure 1. Structure of 2-aminopurine showing the numbering scheme and the direction of the ground (S_0) state dipole moments for the C_1 symmetry (—) and C_s symmetry (- − -) structures computed for the MP2/6-31G(d,p) optimized geometries using the MP2 density. The reference axis is collinear with the C_4-C_5 bond and the in-plane angle (ϕ) is shown. The dipole moment moment for the C_1 structure is tipped by ∼10° out of the plane of the ring.

Solvation Effects. Solvation effects on the absorption and emission transitions of 2AP were taken into account using the Onsager model,[23] which considers the dipolar interaction of a spherical cavity containing the solute dipole with the reaction field of a dielectric continuum, which is characterized by its refractive index and static dielectric constant. The cavity radius was chosen to be 3.77 Å, which is the value used by Broo and Holmén in their MP2 calculations of ground state 2AP and adenine.[17] This value was determined using the mass−density method of Karelson and Zerner.[24] We assume that the size of the cavity is independent of the size of the basis set. In addition, the use of the same cavity radius to estimate the solvation energies for both ground and excited states presumes that the electronic spatial extent (i.e., $\langle r^2 \rangle$) for the ground and excited states is similar. This is reasonable given that we are are only considering low-lying valence states. Solvation effects on the ground and excited geometries were not considered.

Results and Discussion

Ground State Structure. The similarity of the MP2/6-31G-(d) and DFT/6-311++G(df,p) calculations of the ground state structure of 2AP from ref 17 suggested that the computed bond angles and distances are relatively insensitive to the presence of diffuse functions in the basis set. We have carried out geometry optimizations of both planar and nonplanar 2AP using MP2/6-31G(d,p), which places polarization functions on both the hydrogens and heavy atoms. In addition, we have also determined the RHF/6-31G(d,p) geometry, which, when compared to the MP2 geometry, allows us to gauge the influence of electron correlation effects on the ground state structure. Knowledge of the role of correlation effects will be important in comparing the energy-minimized geometries of the S_0 state with that obtained for the S_1 state obtained using the CIS method (vide infra).

Figure 1 shows the structure of 2AP and the orientation of the computed dipole moments, obtained using the MP2 density, in the plane of the purine ring for both the planar and nonplanar structures. In the case of the C_1 structure, the pyramidal geometry of the amino group leads to tipping of the dipole out of the plane by approximately 10°. The computed ground state energies, dipole moments, bond angles and distances, and dihedral angles defining the amino group geometry for both the planar and nonplanar structures are shown in Table 1. The ring geometry obtained for C_1 symmetry at the MP2/6-31G-(d,p) level is nearly identical to the published geometry obtained

TABLE 1: Ground State Energies, Dipole Moments, and Structural Parameters of 2-Aminopurine

	C_1(MP2/ 6-31G(d,p))	C_s(RHF/ 6-31G(d,p))	C_s(MP2/ 6-31G(d,p))
energy (au)	−465.9870	−464.5349	−465.9859
μ (D)	3.33	3.07	3.14
ϕ (deg)[a]	30.5	20.2	20.5
Bond Distances (Å)			
N_1-C_2	1.362	1.342	1.364
C_2-N_3	1.344	1.327	1.346
C_2-N_{10}	1.379	1.346	1.362
$N_{10}-H_{11(12)}$	1.007	0.990	1.002
N_3-C_4	1.335	1.315	1.335
C_4-C_5	1.407	1.390	1.407
C_5-N_6	1.397	1.381	1.397
N_1-C_6	1.334	1.311	1.333
C_6-H	1.084	1.077	1.085
C_5-N_7	1.385	1.388	1.386
N_7-C_8	1.321	1.277	1.321
C_8-H	1.079	1.072	1.078
C_8-N_9	1.378	1.378	1.378
C_4-N_9	1.375	1.356	1.375
N_9-H	1.008	0.993	1.007
Bond Angles (deg)			
$N_1-C_2-N_3$	127.8	127.0	127.9
$N_1-C_2-N_{10}$	115.3	115.9	115.2
$N_{10}-C_2-N_3$	116.8	117.0	116.9
$C_2-N_3-C_4$	111.7	112.7	111.6
$N_3-C_4-C_5$	126.8	126.3	126.9
$C_4-C_5-C_6$	115.4	115.2	115.4
$C_5-C_6-N_1$	120.3	120.6	120.4
$C_6-N_1-C_2$	117.9	118.7	117.8
$N_3-C_4-N_9$	128.5	128.7	128.4
$C_4-C_5-N_7$	111.4	110.4	111.5
$C_5-N_7-C_8$	103.4	104.4	103.4
$N_7-C_8-N_9$	113.9	113.9	113.9
$N_8-N_9-C_4$	106.5	106.3	106.6
Amino Group Dihedrals (deg)			
$C_6-N_1-C_2-N_{10}$	−176.3	180.0	180.0
$N_1-C_2-N_{10}-H_{11}$	−20.9	0.0	0.0
$H_{12}-N_{10}-C_2-N_3$	21.2	0.0	0.0
$N_{10}-C_2-N_3-C_4$	−176.1	180.0	180.0

[a] Angle between dipole moment and reference axis defined in Figure 1.

at the MP2/6-31G(d) level. Typical differences between the calculated bond distances and angles for the purine ring are <0.002 Å and <0.1°, respectively. The degree of pyramidalization of the amino group in the MP2/6-31G(d,p) calculation is slightly greater than that obtained by Broo and Holmén. For example, our result for the $N_1-C_2-N_{10}-H_{11}$ dihedral angle is −20.9° compared to their value of −16.9°. We attribute this difference to the presence of p-type functions on the amino hydrogens in our basis set. Comparison of the MP2/6-31G(d,p) geometries for the C_1 and C_s symmetry structures shows that constraining the amino group to lie in the plane of the ring has little effect on the ring geometry. Larger structural differences are seen in comparing the RHF/6-31G(d,p) and MP2/6-31G(d,p) results for the C_s structure, where deviations as large as 0.02 Å and 1° are found for the bond distances and bond angles, respectively. The most obvious trend in these differences is that the inclusion of correlation effects leads to increased bond distances.

As noted earlier, the influence of base−base interactions in a nucleic acid may lead to increasing planarity of the amino group. As can be seen from Table 1, the difference in energies for the fully optimized C_1 and C_s structures obtained at the MP2/6-31G(d,p) level is only approximately 250 cm^{-1}. Stewart et al. in their ab initio studies of adenine found a similar result.[25] In addition, constraining the amino group and ring system to be planar leads to very small differences in the values of the ring bond distances and bond angles. For the excited state calculations presented here, we used the ground state geometries for the planar and nonplanar structures obtained from the MP2/6-31G(d,p) optimization.

Vertical Transitions From the S_0 State. We have employed a series of double-ζ and triple-ζ basis sets with and without both p- and d-type (polarization) functions on the heavy atoms and diffuse sp-type functions in calculating the excitation energies, transition dipole moments, and permanent dipole moments of the three lowest-lying valence excited states of both C_1 and C_s 2AP. The size of the basis sets ranged from 160 to 255 basis functions. For each structure, basis sets containing diffuse functions produced one or more low-lying virtual orbitals with considerable atomic character. For these basis sets, a state with Rydberg character was predicted to fall between the lowest $\pi-\pi^*$ and $n-\pi^*$ states. The energy of this state showed much more sensitivity to basis size than did the valence states. In what follows we consider only the excited valence states.

The excited state transition energies, oscillator strengths, transition dipole directions, and permanent dipole moments for both C_1 and C_s structures are shown in Table 2 along with the experimental values for comparison. The computed values correspond to excited states that can be reached via vertical excitation from the ground state minimum and, in the spirit of the classical Franck principle, are related to the final state accessed in an absorption process. As can be seen in the table, the use of a double-ζ basis set with both polarization and diffuse functions (e.g., 6-31+G(d)) produced values for each of the excited state properties that are nearly converged. Addition of a second set of diffuse functions to a double-ζ basis (6-31++G(d)) produced only very minor changes to any of the computed properties. The triple-ζ 6-311++G(d) basis produced transition energies that were a few hundredths of an electonvolt lower than those obtained at the 6-31++G(d) level and transition dipole moments that differed in their orientation by 1−2°. Addition of polarization functions to the hydrogens in a triple-ζ basis (6-311++G(d,p); data not shown) left the values for each of the properties essentially unchanged.

In comparing the ab initio results with those obtained experimentally, the most notable discrepancies are the excitation energies, which are substantially overestimated in the CIS calculations. The overestimation of transition energies is common in calculations with this method and is a result of limiting the description of the excited state wave function to singly excited configurations. This procedure fails to properly account for differences in dynamical electron correlation in the ground and excited states. Broo and Holmén have suggested that this difference is comparable in all the nucleobases and have used a scaling factor of 0.72 for the excitation energies of the $\pi-\pi^*$ transitions.[26] Multiplication of the CIS/6311++G(d) $S_0 \rightarrow S_1$ excitation energy by this factor yields a value of 31 960 cm^{-1} compared with the experimental value of 32 800 cm^{-1}.

While the excitation energies for the $\pi-\pi^*$ and $n-\pi^*$ states converge in the CIS method to values that are significantly higher than the experimental values, the excited-state energy gaps for the three lowest-lying states and the transition dipole directions for the $\pi-\pi^*$ transitions are in general agreement with those obtained experimentally.[14] The calculated energy gaps for 2AP in vacuo along with the experimental results of 2AP in PVA are shown in Figure 2a. The gap between the S_1 and S_2 states in C_1 symmetry obtained using CIS is 6200 cm^{-1} compared to the experimental value of ∼3200 cm^{-1}. It should

TABLE 2: Basis Set Dependence of Excited State Electronic Properties of Isolated 2-Aminopurine

symmetry	state	assign[a]	6-31G(d)	6-31+G(d)	6-31++G(d)	6-311++G(d)	exptl
C_1	S_1	$\pi-\pi^*$	$E/cm^{-1} = 46165$	44719	44704	44385	32800
			$f^b = 0.31$	0.32	0.32	0.31	0.10
			$\theta^c = 67°$	68°	68°	67°	55°
			$\mu/D^d = 4.22$	4.38	4.35	4.34	
			$\phi^e = 24°$	22°	22°	22°	
	S_2	$n-\pi^*$	$E/cm^{-1} = 51062$	50756	50748	50630	~36000
			$\phi = 0.006$	0.005	0.005	0.005	~0.002
			$\theta = \perp^f$	$\perp$	$\perp$	$\perp$	$\perp$
	S_3	$\pi-\pi^*$	$E/cm^{-1} = 53214$	51990	52008	51756	40000
			$f = 0.13$	0.13	0.12	0.13	0.06
			$\theta = -78°$	−76°	−76°	−75°	−70°
C_s	S_1	$\pi-\pi^*$	$E/cm^{-1} = 45635$	44136	44125	43820	
			$f = 0.31$	0.33	0.32	0.31	
			$\theta = 67°$	67°	66°	66°	
			$\mu/D = 4.25$	4.49	4.49	4.49	
			$\phi = 14°$	11°	11°	11°	
	S_2	$n-\pi^*$	$E/cm^{-1} = 51248$	50901	50908	50755	
			$f = 0.006$	0.005	0.006	0.006	
			$\theta = \perp$	$\perp$	$\perp$	$\perp$	
	S_3	$\pi-\pi^*$	$E/cm^{-1} = 53521$	52006	51996	51752	
			$f = 0.13$	0.13	0.12	0.13	
			$\theta = -78°$	−76°	−76°	−75°	

[a] The labeling of states as $n-\pi^*$ and $\pi-\pi^*$ is only approximate in C_1 symmetry. [b] Oscillator strength. [c] Angle between transition dipole moment and reference axis defined in Figure 1. [d] Permanent dipole moment in debyes. [e] Angle between permanent dipole moment and reference axis. [f] Perpendicular to the plane of the purine ring.

be noted that the experimental value for the excitation energy of the $n-\pi^*$ state contains some uncertainty due to its very low oscillator strength and the assumption of pairwise overlapping bands used in fitting the LD spectra. In addition, the possibility exists of vibronic coupling between the weakly allowed $n-\pi^*$ transition and the nearby strongly allowed $\pi-\pi^*$ transitions, which could lead to polarization mixing further obscuring the location of the $n-\pi^*$ state. The computed gap between the two low-lying $\pi-\pi^*$ states is 7400 cm^{-1}, in excellent agreement with the experimental value of 7200 cm^{-1}. The INDO/S results obtained for 2AP in vacuo predict $S_1 \rightarrow S_2$ and $S_1 \rightarrow S_3$ gaps of ~600 and 4550 cm^{-1}, respectively.[14]

The oscillator strengths for the three lowest-lying transitions are also substantially overestimated (by about a factor of 3) by both the CIS and INDO/S calculations. The distribution of oscillator strength among the $\pi-\pi^*$ states, however, is modeled quite accurately by the CIS method. The ratio of oscillator strengths, $S_0 \rightarrow S_1/S_0 \rightarrow S_2$, obtained via CIS is ~53 compared to the experimental value of ~50 and the INDO/S value of 21. The $S_0 \rightarrow S_1/S_0 \rightarrow S_3$ value is computed by CIS to be 2.3 compared to the experimental value of 1.7 and the INDO/S value of 0.68. The orientations of the calculated transition dipole moments for the in-plane $\pi-\pi^*$ transitions, shown in Figure 2b, agree well with experimental values, differing by ~12° and 5° for the $S_0 \rightarrow S_1$ and $S_0 \rightarrow S_3$ transitions, respectively, and are similar to those obtained using INDO/S. For both $S_0 \rightarrow S_1$ and $S_0 \rightarrow S_3$ transitions, the ab initio results predict a slightly larger projection of the transition moment along the long axis of the purine ring than is found experimentally.

The magnitude and direction of the permanent dipole moment of the S_1 state of C_1 2AP for the various basis sets is also given in Table 2. The dipole moment for this state is larger in magnitude by 35% than, and oriented nearly parallel to, that of the ground state. In summary, the CIS method overestimates the transition energies and oscillator strengths for the $\pi-\pi^*$ transitions but yields excited state energy gaps, transition dipole directions, and relative oscillator strengths that are in substantial agreement with the experimental results.

We can also examine the influence of the amino group conformation on the excited state energetics and properties of 2AP by comparing the results obtained for the C_1 and C_s symmetry structures. Comparison of the results summarized in Table 2 shows that distortion of the amino group to lie in the plane of the purine ring leads to a slight (550 cm^{-1}) lowering of the $S_0 \rightarrow S_1$ excitation energy. The excitation energies of the S_2 and S_3 states are much less sensitive to this distortion, with the result that the gap between the lowest-lying $\pi-\pi^*$ state and the $n-\pi^*$ state is increased to approximately 6900 cm^{-1}. Assuming that stacking of 2AP in a nucleic acid leads to a flattening of the amino group, one could, in principle, use the resulting red shift in the $\pi-\pi^*$ absorption transition as a reporter of the extent of stacking; however, the small value of the predicted shift (~6 nm) coupled with the fact that the 2AP transition appears as a weak shoulder on the red edge of the nucleic acid absorption makes it doubtful that such a shift could be resolved.

The orientation of the two $\pi-\pi^*$ transition dipole moments in the plane of the ring differ by only ~1° for the two geometries. The permanent dipole moment of the S_1 state is slightly more affected by amino group planarity. The S_1 dipole moment obtained for the C_s structure is lower in magnitude by about 3% and rotated in the plane by 11° from that of the C_1 structure.

Vertical Transitions from the S_1 State. Within the classical Franck principle, fluorescence is a vertical process originating from the minimum of the S_1 potential surface. The energy gap between the ground and fluorescent $\pi-\pi^*$ state potential minima closely approximates the observed fluorescence maximum. To estimate the red shift of the fluorescence from the $S_0 \rightarrow S_1$ absorption maximum, we have carried out CIS calculations of the $S_1 \rightarrow S_0$ energy gap at the minimum of the S_1 potential, obtained from a geometry optimization of this state at the CIS/6-31G(d,p) level. A similar calculation of the excited state geometry using a double-ζ basis with diffuse functions (6-31+G(d,p)) yielded a structure that was essentially identical to the one obtained with the 6-31G(d,p) basis. For each basis set, the optimized S_1 state was found to be essentially planar (deviations of the dihedral angles from planarity were less that 0.05°), in agreement with ab initio results employing smaller basis sets.[15] The excited state bond distances and bond angles are shown in Table 3.

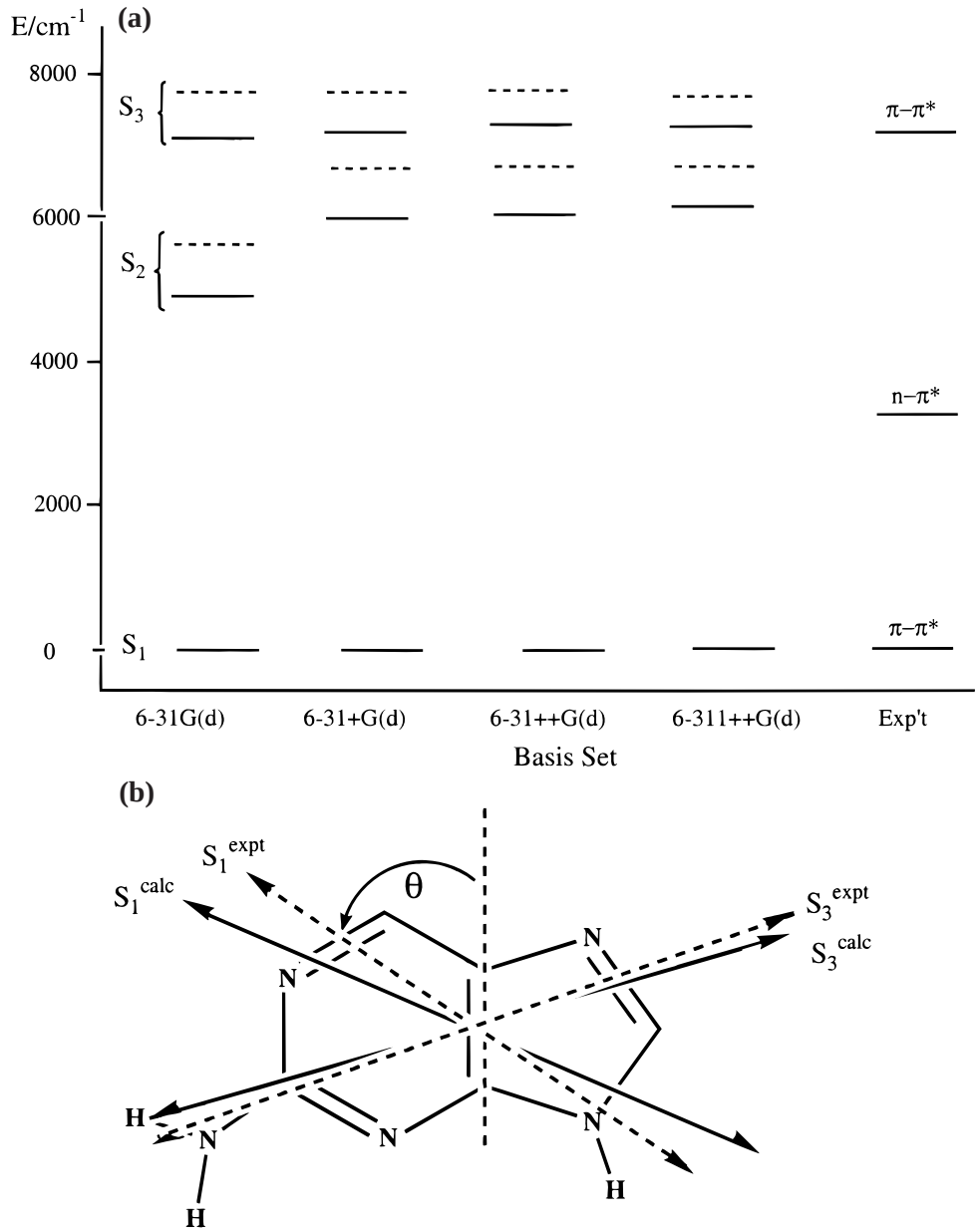

Figure 2. (a) Vertical energy level diagram obtained using the ground-state optimized geometries for the three lowest-lying valence states of 2AP as a function of basis set: (—) C_1 symmetry; (- − -) C_s symmetry. The experimental results are taken from ref 14. (b) Transition dipole directions for the $S_0 \rightarrow S_1$ ($\pi-\pi^*$) and $S_0 \rightarrow S_3$ ($\pi-\pi^*$) transitions of 2AP (C_s structure) computed at the CIS/6-311++G(d) level and the corresponding directions obtained from linear dichroism experiments (ref 14).

TABLE 3: Geometry of the S_1 State of 2-Aminopurine Obtained at the CIS/6-31G(d,p) Level

Bond Distances (Å)		Bond Angles (deg)	
N_1-C_2	1.323	$N_1-C_2-N_3$	129.9
C_2-N_3	1.385	$N_1-C_2-N_{10}$	117.0
C_2-N_{10}	1.334	$N_{10}-C_2-N_3$	113.1
$N_{10}-H_{11(12)}$	0.990	$C_2-N_3-C_4$	109.5
N_3-C_4	1.311	$N_3-C_4-C_5$	127.3
C_4-C_5	1.428	$C_4-C_5-C_6$	116.9
C_5-N_6	1.426	$C_5-C_6-N_1$	116.7
N_1-C_6	1.346	$C_6-N_1-C_2$	119.4
C_6-H	1.071	$N_3-C_4-N_9$	128.4
C_5-N_7	1.345	$C_4-C_5-N_7$	110.0
N_7-C_8	1.315	$C_5-N_7-C_8$	105.7
C_8-H	1.070	$N_7-C_8-N_9$	112.9
C_8-N_9	1.355	$N_8-N_9-C_4$	107.2
C_4-N_9	1.366		
N_9-H	0.993		

Using the 6-311++G(d) basis set, the vertical $S_1 \rightarrow S_0$ transition energy from the relaxed (planar) excited state is predicted to occur at 40 345 cm^{-1} (248 nm). Comparison of this value with that for the vertical $S_0 \rightarrow S_1$ transition obtained at the S_0 geometry using the same basis set gives a red shift of ~4040 cm^{-1} for 2AP fluorescence in vacuo. This represents the reorganization energy associated with relaxation of the structure arising from differences in the ground and excited state force fields in the absorption and emission processes. The nature of this structural change can be seen by comparing the geometries obtained using the 6-31G(d,p) basis for the S_0 and S_1 states. In making this comparison, it seems more reasonable to use the S_0 geometry obtained without correlation corrections (i.e., RHF/6-31G(d,p)), because electron correlation is not treated to the same extent in the CIS method as in the MP2 method. In addition to increasing planarity of the amino group, several ring coordinates also undergo distortion upon excitation to the $\pi-\pi^*$ state. While no attempt has been made to calculate normal coordinate displacements between the S_0 and S_1 states, comparison of the bond angles and distances of the two geometries

shows that considerable lengthening of the N_7-C_8 bond in the five-membered ring occurs as well as distortion of the six-membered ring along the *y*-axis leading to increases in the N_1-C_6, C_2-N_3, and C_4-C_5 bond distances and concomitant decreases in the $C_2-N_3-C_4$ and $N_1-C_6-C_5$ bond angles, thus vibrational modes with large projections onto these local displacements would be expected to couple to the electronic excitation. We note that similar conclusions are reached in comparing the S_1 geometry with the S_0 geometry obtained from the MP2 method.

It is important to consider the energy gap between the S_1 and S_2 ($n-\pi^*$) states at the S_1 minimum. Close proximity of these two states at the geometry of the relaxed S_1 state would suggest the possibility of nonradiative relaxation to the non-emitting $n-\pi^*$ state in the planar structure. We find that the gap between S_1 and S_2 is slightly larger (7160 cm^{-1}) at the S_1 state minimum than at the S_0 minimum, precluding any influence of the S_2 state on the photophysics of the S_1 state. We note that this is in contrast to the situation found in adenine. Calculations by Broo show that for the 9-H tautomer, the $\pi-\pi^*$ and $n-\pi^*$ states cross near the minimum of the $\pi-\pi^*$ state.[15]

Solvation Effects on the Absorption and Emission Spectra. To investigate the influence of dipolar solvation on the $S_0 \rightarrow S_1$ transition in both absorption and emission, we work within the basic framework of the Onsager model.[23] In this approach, the solvation energy (defined as the energy of the solvated species minus that of the isolated species) is estimated by considering the interaction of a spherical cavity of radius a_o containing the solute dipole moment with the reaction field of the solvent, which is represented as a dielectric continuum. The solvation energy of state *i* is given by $E_i^{solv} = -\mu_i R$, where μ_i is the dipole moment of the *i*th state and *R* the solvent reaction field. The reaction field depends on the magnitude and direction of the dipole moment giving rise to the solvent polarization. In considering solvent effects on absorption and emission processes, the separate contributions to the solvation energies of the two electronic states by the fast (electronic) and slow (orientational) solvent response must be taken into account. In absorption, the initial (ground) state is fully solvent equilibrated, and the reaction field is given by $R = (2\mu_o/a_o^3)\{(\epsilon - 1)/(2\epsilon + 1)\}$, where ϵ is the static dielectric constant of the solvent. The solvation energy of the ground state is thus

$$E_o^{solv} = -\frac{2}{a_o^3}\vec{\mu}_o \cdot \vec{\mu}_o \left\{\frac{\epsilon - 1}{2\epsilon + 1}\right\} \quad (1)$$

The vertical transition is to an S_1 state in which only the electronic response is realized; thus, the reaction field felt by the final state arising from the orientational part of the solvent polarization is that corresponding to the fully relaxed ground state. The solvation energy of the S_1 state in the absorptive process is thus given by

$$E_1^{solv} = -\frac{2}{a_o^3}\left[\vec{\mu}_1 \cdot \vec{\mu}_o \left\{\frac{\epsilon - 1}{2\epsilon + 1} - \frac{n^2 - 1}{2n^2 + 1}\right\} + \vec{\mu}_1 \cdot \vec{\mu}_1 \left\{\frac{n^2 - 1}{2n^2 + 1}\right\}\right] \quad (2)$$

where *n* is the solvent refractive index. The two terms on the right-hand side of eq 2 reflect the contributions from the orientational and electronic solvent responses, respectively. It is important to note that this nonrelaxed solvation energy depends not only on the magnitudes of the ground and excited state dipole moments but also on the angle between them. The vertical $S_0 \rightarrow S_1$ excitation energy in solution is

$$E_{0\rightarrow 1}^{sol} = E_{0\rightarrow 1}^{gas} + E_1^{solv} - E_0^{solv} \quad (3)$$

In the emission process the situation is reversed. Assuming that the solvent longitudinal relaxation time is much shorter than the S_1 lifetime, the excited state is fully relaxed and the final (ground) state experiences the orientational reaction field corresponding to the dipole moment of the S_1 state. The $S_1 \rightarrow S_0$ transition energy in solution can thus be obtained from eq 3 and by switching the 0 and 1 subscripts in eqns 1 and 2.

A standard procedure for estimating solvation energies for an electronic state is to incorporate the reaction field into the isolated molecule Hamiltonian as a perturbative term and solve for the solvation energy in an iterative fashion. This is known as the Onsager self-consistent reaction field (SCRF) method and takes into account the polarizing influence of the solvent reaction field on the solute dipole moment.[27,28] Interaction of the reaction field and solute dipole can lead to significant differences between the dipole moment of the gas phase and solvated species. While the SCRF method is available in Gaussian 94, the dielectric continuum in this program is parametrized by only the static dielectric constant; thus it is not possible to directly generate the solvent effect for a vertical transition via the CIS method. Our approach to implementing eq 3 is to employ the Onsager SCRF method to calculate the dipole moments of the S_0 and S_1 states at the appropriate geometries using the 6-311++G(d) basis. The ground and excited state dipole moments are then used to calculate the relevant solvation energies via eqs 1 and 2. Our calculations take into account the effect of intramolecular (vibrational) relaxation on the dipole moments of both states (i.e., the dipole moments of the S_1 state at the S_0 and S_1 minima differ slightly mainly due to differences in the amino group geometry in the relaxed ground and excited states). The gas-phase transition energies are those obtained using the 6-311++G(d) basis.

Our results for the effect of dipolar solvation on the vertical absorption ($S_0 \rightarrow S_1$) and emission ($S_1 \rightarrow S_0$) transition energies along with the dipole moments obtained using the SCRF procedure and the dielectric constant for water ($\epsilon = 78.0$) are shown in Table 4. For the ground state, the SCF density was used to compute the dipole moments at the geometries corresponding to the S_0 and S_1 minima. The CIS density was used to compute the excited state dipole moments. The dipole moments for both ground and excited states increase in magnitude by approximately 30% in going from gas phase to solution. In the case of the absorption spectrum, the difference between the solvation energies for the ground and excited states (at the S_0 minimum) gives rise to a calculated solvent shift of -810 cm^{-1}.

Also shown in Table 4 are the solvation energies for the S_0 and S_1 states obtained using the dipole moments corresponding to the S_1 state potential minimum. The computed solvent shifts in this case are -1405 and -3480 cm^{-1} for the ground and excited states, respectively. The difference in the values for the solvation energies for the S_0 and S_1 states in absorption and emission reflects the different contributions of the high- and low-frequency responses in absorption and emission.

From the values for the $S_0 \rightarrow S_1$ and $S_1 \rightarrow S_0$ transition energies in Table 4, we find that the fluorescence Stokes' shift in water is calculated to be $\sim$5305 cm^{-1}. The experimental value in water is $\sim$5200 cm^{-1}.[3] If we scale our result for the $S_0 \rightarrow S_1$ transition in absorption to agree with the experimental value of 32 800 ($\lambda = 305$ nm), the computed Stokes' shift places the emission maximum at 364 nm, compared to the experimental value of $\sim$360 nm.[3] In our calculation, the component of the

TABLE 4: S_0 and S_1 Dipole Moments, Solvation Energies, and Vertical Transition Energies Obtained Using the 6-311++G(d) Basis Set (Energies are in cm^{-1})

state	μ/D[a]	ϕ[b] (ϕ')[c]	E^{solv}	$E^{gas}_{0\rightarrow1}$	$E^{soln}_{0\rightarrow1}$
absorption[d]					
S_0	4.50	35°(12°)	−1830	44385	43575
S_1	6.18	24°(11°)	−2640		
emission[e]					
S_0	4.05	23°(∼0°)	−1405	40345	38270
S_1	6.12	12°(∼0°)	−3480		

[a] Permanent dipole calculated using Onsager SCRF method with $\epsilon = 78.0$. [b] Angle between the dipole moment and reference axis shown in Figure 1. [c] Angle between the dipole moment and the plane of the ring. [d] Dipole moments computed from the Hartree−Fock density using the ground-state geometry optimized at the MP2/6-31G(d,p) level. [e] Dipole moments computed from the CIS density using the S_1 geometry optimized at the CIS/6-31G(d,p) level.

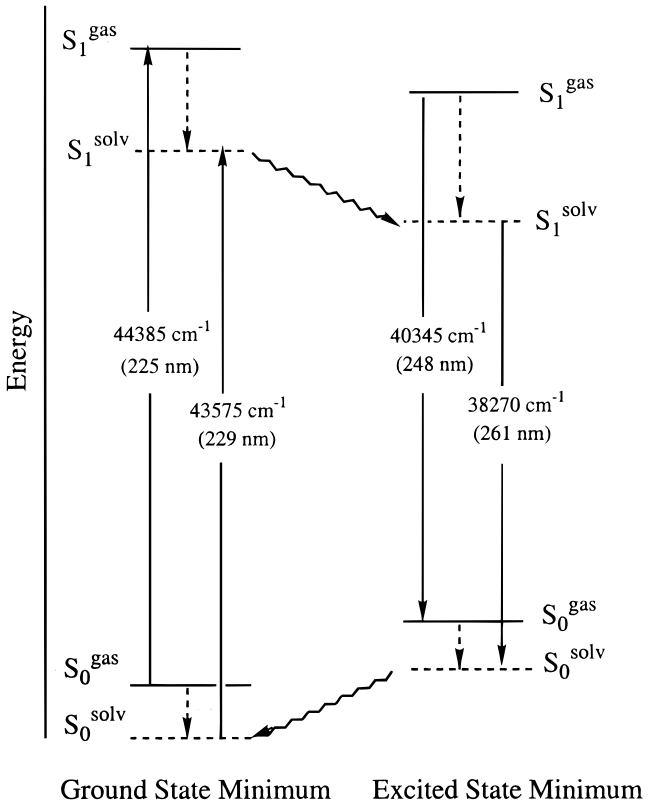

Figure 3. Jablonski diagram showing the S_0 and S_1 states of 2AP and the vertical transitions in absorption and emission for both the isolated and solvated species as calculated using the CIS method and Onsager model. Dashed lines with arrows denote the relevant solvation processes in absorption and emission. Wavy lines correspond to orientational relaxation of the solvent and intramolecular vibrational relaxation.

Stokes' shift arising from solvent reorganization is quite small (1265 cm^{-1}). This is due to the fact that although excitation from S_0 to S_1 results in an increase of almost 50% in the magnitude of the dipole moment, the orientation of the two dipoles changes by only ∼12°; thus little solvent reorganization occurs as a result. These results are summarized in the energy level diagram of Figure 3, which shows the vertical transitions in absorption (ground-state minimum) and emission (excited-state minimum) for both the isolated and solvated species. In the diagram, the dashed arrows connecting the gas phase and solvated initial states in the absorption and emission processes correspond to the solvation energies arising from the full solvent response to the permanent dipole moment of the initial state involved in the transition. The remaining two arrows denote the solvation energies obtained for the final states in absorption and emission. The orientational contributions to these solvation energies arise from the equilibrium solvent configurations corresponding to the initial states in the transitions. The wavy arrows denote the nuclear dynamics that occur following the "instantaneous" vertical transitions (i.e., vibrational relaxation and solvent reorganization). As is evident from the diagram, the fluorescence Stokes' shift is the sum of the nuclear contributions to the solvation energies of the ground and excited states.

Though our calculation of the Stokes' shift is in excellent agreement with the experimental value, several caveats regarding potential sources of error merit mention. Errors in the solvent contribution to the Stokes' shift may arise from (i) specific solvent effects not included in the Onsager model, (ii) inherent limitations of the Onsager model, and/or (iii) inherent limitations of the CIS method to produce accurate values for permanent dipole moments of excited states. With regard to specific solvent effects, the INDO/S SCRF calculations on the 2AP/water cluster suggest that hydrogen bonding has a very minor effect on the absorption spectrum.[14] We would not expect hydrogen bonding to have a substantial influence on the $\pi-\pi^*$ transition; however, the $n-\pi^*$ state may be considerably more affected by such specific solvent interactions. The limitations of the Onsager model include truncation of the electrostatic interaction between the cavity and the reaction field at the dipole level and the use of a spherical cavity for an obviously nonspherical molecule. Recent calculations, however, showed that this combination of assumptions produces errors in solvation energies that fortuitously cancel to a large extent.[29] While other dielectric continuum models exist, which relax the Onsager assumptions, it is not yet clear which, if any, of these is superior given the uncertainties in choosing the cavity size and shape.

An obvious limitation of CIS is the treatment of electron correlation in this method. The extent to which correlation effects influence the excited state charge distribution is not easily ascertained. We can gauge the effect of electron correlation on the ground state charge distribution, however, by comparing the gas-phase dipole moments computed at the restricted Hartree−Fock and MP2 levels using the MP2/6-31G(d,p) optimized geometries shown in Table 1. We find that inclusion of correlation to second order changes the magnitude of the ground state dipole moment by only about 1% and the orientation by 1°. Such changes in the excited-state dipole moments would have negligible effect on the computed solvation energies.

The small value for the solvent contribution to the Stokes' shift suggests that the fluorescence maximum of 2AP is relatively insensitive to the polarity of the environment. This is contrast to the case of tryptophan, for example, where the large dipole moment change accompanying excitation to the L_a state gives rise to a fluorescence spectrum whose maximum wavelength provides a sensitive reporter of the polarity of the local environment.[30,31]

We note that more sophisticated methods for incorporating correlation effects in computing spectra, such as CASPT2[32] and time-dependent DFT,[33,34] may yield more accurate transition energies; however, the excited state energy gaps and transition dipole directions obtained using CIS generally agree well with experiment suggesting the CIS method is appropriate for these properties and for estimating the effects of solvation on the transition energies. In addition, the computational efficiency of CIS makes possible the extension of the method to the study of the excited state properties of 2AP-containing dinucleotides and

trinucleotides. Such studies are currently underway and should allow us to understand the effects of base−base interactions on the excited-state properties of 2AP.

Summary

Extensive calculations of the electronically excited-state manifold and properties of 2AP in both planar and nonplanar geometries have been carried out using the CIS method with moderate to large basis sets. Excited state vertical excitation energies and transition dipole moments for the three lowest-lying valence transitions were obtained at both the S_0 and S_1 state potential minima. While the excitation energies are consistently overestimated, the excited-state energy gaps and transition dipole directions are in good agreement with those obtained for 2AP in PVA films. In addition, we have calculated the permanent dipole moments for the S_0 and S_1 states and used these to determine the solvation energies (in water) for each state in both absorption and emission using the Onsager reaction field model. The computed Stokes' shift is in excellent agreement with that obtained experimentally and the results suggest that the majority of the Stokes' shift in an aqueous environment arises from vibrational relaxation rather than solvent reorganization.

Acknowledgment. This work was supported by the NSF (to K.B.H.). We thank the Washington University Department of Chemistry Computer Facility for computer access.

References and Notes

(1) Nordlund, T. M.; Andersson, S.; Nilsson, L.; Rigler, R.; Gräslund, A.; McLaughlin, L. W. *Biochemistry* **1989**, *28*, 9095.
(2) Scheit, K. H.; Rackwitz, H. R. *Nucleic Acids Res*. **1982**, *10*, 459.
(3) Ward, D. C.; Reich, E.; Stryer, L. *J. Biol. Chem.* **1969**, *244*, 1228.
(4) Gräslund, A.; Claesens, F.; McLaughlin, L. W.; Lycksell, P.-B.; Larsson, U.; Rigler, R. *In Structure, Dynamics and Function of Biomolecules, Springer Series in Biophysics*; Ehrenberg, A., Rigler, R., Gräslund, A., Nilsson, L., Eds.; Springer-Verlag: Berlin, 1987; Vol. 1, p 201.
(5) Menger, M.; Tuschl, T.; Eckstein, F.; Porschke, D. *Biochemistry* **1996**, *35*, 14710.
(6) Guest, C. R.; Hochstrasser, R. A.; Sowers, L. C.; Millar, D. P. *Biochemistry* **1991**, *30*, 3271.
(7) Stivers, J. T. *Nucleic Acids Res.* **1998**, *26*, 3837.
(8) Nordlund, T. M.; Xu, D. E.; Evans, K. O. *Biochemistry* **1993**, *32*, 12090.
(9) Law, S. M.; Eritja, R.; Goodman, M. F.; Breslauer, K. J. *Biochemistry* **1996**, *35*, 12329.
(10) Watanabe, S. M.; Goodman, M. F. *Proc. Natl Acad. Sci*. **1981**, *78*, 2864.
(11) Fagan, P. A.; Fabrega, C.; Eritja, R.; Goodman, M. F.; Wemmer, D. E. *Biochemistry* **1996**, *35*, 4026.
(12) Sowers, L. C.; Fazakerley, G. V.; Eritja, R.; Kaplan, B. E.; Goodman, M. F. *Proc. Natl. Acad. Sci.* **1986**, *83*, 5434.
(13) Laughlin, L. W.; Leong, T.; Benseler, F.; Piel, N. *Nucleic Acids Res.* **1988**, *16*, 5631.
(14) Holmén, A.; Nordén, B.; Albinsson, B. *J. Am. Chem. Soc*. **1997**, *119*, 3114.
(15) Broo, A. *J. Phys. Chem. A* **1998**, *102*, 526.
(16) Harnden, M. R.; Jarvest, R. L.; Slawin, A. M. Z.; Williams, D. J. *Nucleosides Nucleotides* **1990**, *9*, 499.
(17) Broo, A.; Holmén, A. *Chem. Phys.* **1996**, *211*, 147.
(18) Callis, P. *Annu. Rev. Phys. Chem*. **1983**, *34*, 329.
(19) Wilson, R. W.; Callis, P. R. *Photochem. Photobiol*. **1980**, *31*, 323.
(20) Santhosh, C.; Mishra, P. C. *Spectrochim. Acta* **1991**, *75*, 407.
(21) Foresman, J. B.; Head-Gordon, M.; Pople, J. A.; Frisch, M. J. *J. Phys. Chem*. **1992**, *96*, 135.
(22) Frisch, M. J.; Trucks, G. W.; Head-Gordon, M.; Gill, P. M. W.; Wong, M. W.; Foresman, J. B.; Johnson, B. G.; Schlegel, H. B.; Robb, M. A.; Replogle, E. S.; Gomperts, R.; Andres, J. L.; Raghavachari, K.; Binkley, J. S.; Gonzalez, C. S.; Martin, R. L.; Fox, D. J.; Defrees, D. J.; Baker, J.; Stewart, J. J. P.; Pople, J. A. *Gaussian 94*; Gaussian, Inc.: Pittsburgh, PA, 1996.
(23) Onsager, L. *J. Am. Chem. Soc*. **1938**, *58*, 1486.
(24) Karelson, M. M.; Zerner, M. C. *J. Phys. Chem.* **1992**, *96*, 6949.
(25) Stewart, E. L.; Foley, C. K.; Allinger, N. L.; Bowen, J. P. *J. Am. Chem. Soc.* **1994**, *116*, 7282.
(26) Broo, A.; Holmén, A. *J. Phys. Chem. A* **1997**, *101*, 3589.
(27) Wong, M. W.; Wiberg, K. B.; Frisch, M. J. *J. Chem. Phys.* **1991**, *95*, 8991.
(28) Wong, M. W.; Frisch, M. J.; Wiberg, K. B. *J Am. Chem. Soc*. **1991**, *113*, 4776.
(29) Foresman, J. B.; Keith, T. A.; Wiberg, K. B.; Snoonian, J.; Frisch, M. J. *J. Phys. Chem.* **1996**, *100*, 16098.
(30) Eftink, M. R. *Methods Biochem. Anal.* **1991**, *35*, 127.
(31) Callis, P. R. *Methods Enzymol*. **1997**, *278*, 113.
(32) Roos, B. O. *Adv. Chem. Phys.* **1987** *69*, 399.
(33) Casida, M. E. In *Recent Advances in Density Functional Methods*; Chong, D. P., Ed.; World Scientific: Singapore, 1995; Vol. 1.
(34) Stratmann, R. E.; Scuseria, G. E.; Frisch, M. J. *J. Chem. Phys.* **1998**, *109*, 8218.